

Green's function retrieval and fluctuations of cross density of states in multiple scattering media

Julien de Rosny*

Institut Langevin, ESPCI, CNRS, 1 rue Vauquelin, 75231 Paris cedex 05

Matthieu Davy

Institut d'Electronique et de Télécommunications de Rennes, University of Rennes 1, Rennes 35042, France

(Dated: 04/09/2013)

Nowadays the noise cross-correlation function (NCF) is widely used to estimate passively the Green's function between two probes. In material science, NCF is also proportional to the cross density of states (CDOS). Here, the average and the variance of the NCF in disordered media are derived in the limits of an equiparted noise field and of a single noise source. We first explain from the ladder approximation, how the diffusion halo plays the role of secondary sources to reconstruct the mean Green's function. Then we show that fluctuations of NCF are governed by several non-Gaussian correlations. The link between these correlations and the intensity ones is highlighted. The infinite-range NCF correlation dominates CDOS fluctuations and proves that NCF is not a self averaging quantity with respect to the plurality of noise sources. Finally for a small number of noise sources, the fluctuations are dominated by local disorder. These results supported by numerical simulations are of importance for passive imaging applications and material science.

A wave propagating in a multiple scattering medium is completely scrambled and generates random intensity patterns. Nevertheless, Weaver and Lobkis[1] showed in 2001 that the time derivative of the cross-correlation of an equipartitioned field measured at two positions \mathbf{r}_A and \mathbf{r}_B is proportionnal to the difference of the causal and anti-causal temporal Green's function (GF). In the frequency domain, the NCF function reduces to the imaginary part of the GF, $\Im G(\mathbf{r}_A, \mathbf{r}_B)$. This result has its roots in the fluctuation-dissipation theorem [2] and has provided a framework for passive imaging systems[3]. It has especially led to spectacular developments in seismology where images of the earth crust have been obtained at different scales with unprecedented resolutions[4, 5]. GF retrieval from cross-correlations of a diffuse field has also been applied to acoustic waves[6], elastic waves[7, 8] and recently electromagnetic waves[9]. The NCF has been interpreted as the field that is back-propagated by a time reversal mirror that completely surrounds a multiple scattering medium[10].

When the positions of the two probes coincide ($\mathbf{r}_A = \mathbf{r}_B$), the cross-correlation becomes the auto-correlation. The auto-correlation linearly depends on the local density of states (LDOS) which counts the number of modes available at a given position. In optics, the LDOS determines spontaneous and stimulated emission of light and is given by $\Im G(\mathbf{r}_A, \mathbf{r}_A)$. LDOS exhibits spatial fluctuations caused by scatterers in the vicinity of the source [11–14]. Indeed, the variance of the LDOS is equal to the C_0 correlation of the intensity [12, 14], which results from local interaction. This infinite spatial range correlation was identified by Shapiro [15]. It differs from the universal intensity correlations C_1 , C_2 and C_3 . The short-range contribution C_1 simply results from Gaussian statistics. The non-Gaussian contributions C_2 and C_3 are

long- and infinite-range contributions, respectively, and enhance intensity fluctuations[16].

About 10 years ago, Van Tiggelen [17] showed that in a random medium, the NCF tends to be self-averaging even though the noise sources are not equally distributed. Because multiple scattering increases the spatial diversity of the field and therefore reduces Gaussian fluctuations, the NCF converges more rapidly towards the average NCF[18]. The same conclusion was derived from a parabolic approximation approach of scattering within the time reversal framework [19]. However, when the distance between \mathbf{r}_A and \mathbf{r}_B is larger than one mean free path (l_e), the mean GF vanishes and the self-averaging property of the NCF seems to be in contradiction with the deterministic approach that claims that the NCF is given by $\Im G(\mathbf{r}_A, \mathbf{r}_B)$. Indeed, even if $\|\mathbf{r}_A - \mathbf{r}_B\| \gg l_e$, $\langle |\Im G(\mathbf{r}_A, \mathbf{r}_B)|^2 \rangle > 0$. This fact means that non-Gaussian correlations should contribute to the NCF fluctuations.

Here we first show that the ladder approximation helps to interpret the emergence of the average NCF in a multiple scattering medium. Scatterers located at one mean free path around the probes play the role of secondary sources. Then using the 8-order diagrammatic expansion of the scattered field, we find the most significant contributions to NCF fluctuations. We derive the analytical expressions of NCF variance for one noise source or a continuous distribution. We show that the same infinite-range correlation causes NCF fluctuations of the cross density of states (CDOS) and explains why the NCF is not self-averaging. The relationship between this infinite-range contribution and the intensity correlations C_0 and C_2 is discussed. All these results are supported by numerical simulations.

We assume a set of uncorrelated wide-band sources of

pink noise represented by the power spectrum function $S_V(\mathbf{r})$ distributed over a volume V (or equivalently a surface in 2D). In the frequency domain, the noise cross correlation ζ_V between two probes at locations \mathbf{r}_A and \mathbf{r}_B is given by,

$$\zeta_V(\mathbf{r}_A, \mathbf{r}_B) = \int G^*(\mathbf{r}_B, \mathbf{r}) G(\mathbf{r}_A, \mathbf{r}) S_V(r) d^d \mathbf{r}. \quad (1)$$

where d is the dimensionality of the space (here 2 or 3). The frequency dependence is kept implicit. When the noise sources are uniformly distributed ($S_V(r) = S_\infty$), the correlation of the field is integrated over the entire scattering volume and the NCF is proportional to the imaginary part of the GF[20],

$$\zeta_\infty(\mathbf{r}_A, \mathbf{r}_B) = -\frac{l_a}{k_0} \Im G(\mathbf{r}_A, \mathbf{r}_B) S_\infty. \quad (2)$$

Here l_a is the absorption (inelastic) mean free path. For finite integration volume, the averaged value of ζ_V can be worked out from multiple scattering theory. The average value $\langle \zeta_V \rangle$ is governed by $\langle G^*(\mathbf{r}_2, \mathbf{r}) G(\mathbf{r}_1, \mathbf{r}) \rangle$. From the Bethe-Salpeter equation and the ladder approximation, the mean NCF is found to be,

$$\begin{aligned} \langle \zeta_V(\mathbf{r}_A, \mathbf{r}_B) \rangle &= \int \langle G(\mathbf{r}_B, \mathbf{r})^* \rangle \langle G(\mathbf{r}_A, \mathbf{r}) \rangle S_V(r) d^d \mathbf{r} \\ &+ \int \langle G(\mathbf{r}_B, \mathbf{r}')^* \rangle \langle G(\mathbf{r}_A, \mathbf{r}') \rangle F(\mathbf{r}') d^d \mathbf{r}' \end{aligned} \quad (3)$$

The halo function $F(\mathbf{r}')$ is equal to $\int | \langle G(\mathbf{r}, \mathbf{r}') \rangle |^2 S_V(r) L(\mathbf{r}', \mathbf{r}') d^d \mathbf{r}'$. The first term in Eq. (3) is the coherent contribution of the field that has not been scattered. The second term is very similar to Eq. (1) where the power spectrum function is replaced by the $F(\mathbf{r}')$. The halo that diffuses from the noise source illuminates the scatterers closer than an elastic mean free path from points A and B. The last scattering events play the role of secondary sources to build up the mean NCF.

To confirm this result, we carry out 2D numerical simulations in the time domain. The scatterers are uniformly distributed inside a ring with an inner radius of $5\lambda_0$ (λ_0 is the central frequency wavelength) and an outer radius of $20\lambda_0$. The mean free path is $\ell_e = 1.5\lambda_0$ and the noise is emitted from a single source outside the multiple scattering medium. The NCF is recorded and averaged over 270 disorder realizations. The time cross-correlation $\langle \zeta_V(\mathbf{r}_A, \mathbf{r}_B, t) \rangle$ which is the inverse Fourier transform of Eq. (3) is shown in Fig. 1 at different times. We clearly observe an almost plane wavefront predicted by the coherent term in (3) as well as a circular wavefront which focuses on point A and is followed by a diverging wavefront. This second contribution appears in a ring around A with a skin depth of about

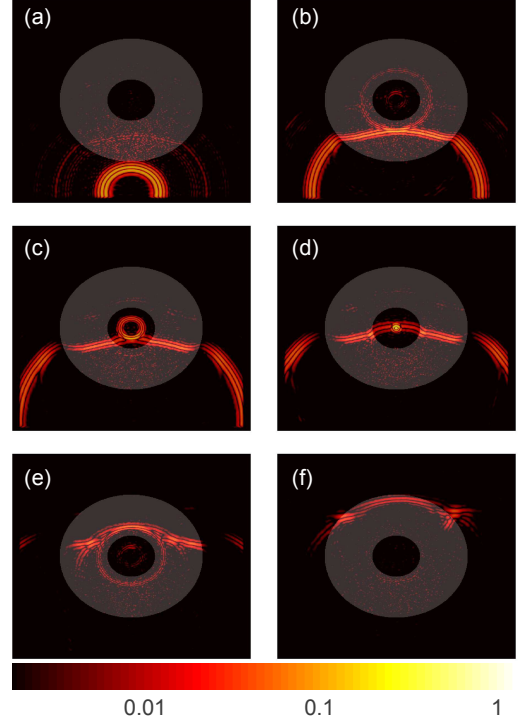


Figure 1. (a)-(f) Average cross-correlated field $\langle \zeta_V(\mathbf{r}_A, \mathbf{r}_B) \rangle$ with respect to \mathbf{r}_B obtained from a finite difference time domain simulation in a multiple scattering media (shown in gray). Point A is at the center of the figure. The 2D simulation domain is a 50 by 50 wavelength square. The noise source is localized at the bottom of the scattering area.

one mean free path. The result is even more spectacular on an animation[21]. This is consistent with (3). Indeed, when the halo is uniformly distributed over at least one mean free path around \mathbf{r}_A and \mathbf{r}_B , $\langle \zeta_V(\mathbf{r}_A, \mathbf{r}_B) \rangle$ is proportional to $\langle G^*(\mathbf{r}_B, \mathbf{r}_A) \rangle - \langle G(\mathbf{r}_B, \mathbf{r}_A) \rangle$ because $\int \langle G(\mathbf{r}, \mathbf{r}_A) \rangle \langle G^*(\mathbf{r}, \mathbf{r}_B) \rangle dV = -\ell_e/k_0 \Im \langle G(\mathbf{r}_B, \mathbf{r}_A) \rangle$ [22] where the mean GF (resp. conjugate mean GF) represents the diverging (resp. converging) coherent wave.

In laboratory experiments, the NCF can easily be averaged over realizations of the disorder. For instance, in optics the scatterers randomly move as a consequence of the Brownian motion. In a microwave experiments, the beads can be mixed in a toner. However, in seismology the NCF can only be measured on a single realization of the disorder. The NCF is expected to be self-averaging[18, 19] as a result of Gaussian statistics. In the context of time reversal[23] or phase-conjugation focusing [24], long range correlations that cannot be predicted by Gaussian fluctuations[25] have been observed. We show in the following how those correlations enhance the fluctuations of the NCF in disordered systems. To this end, we estimated the variance γ of $\zeta_V(\mathbf{r}_A, \mathbf{r}_B)$.

For simplicity, in (1) we have replaced S_V by an integration over a finite volume V . We first consider the case of an equipartitioned diffuse noise, $V \rightarrow \infty$. This

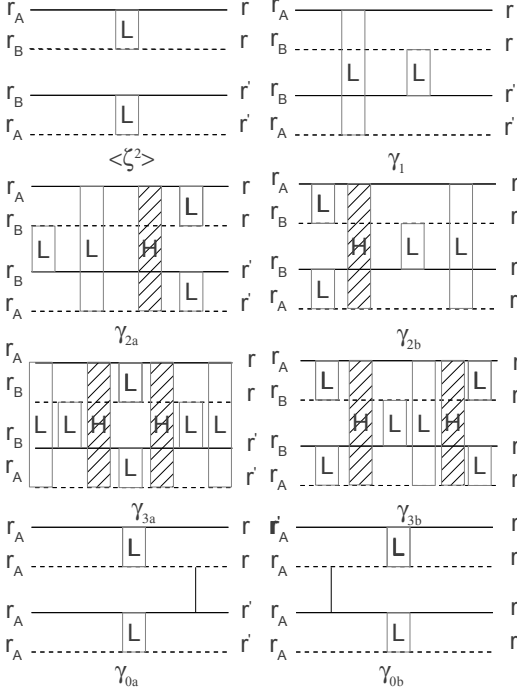


Figure 2. The 8 diagrams that contribute to the variance of the NCF. The symbol L depicts the ladder contribution and H the Hikami box.

is for instance the case of a system at thermal equilibrium. We use a diagrammatic approach to estimate γ in the two limits $\Delta r \gg \ell_e$ and $\Delta r \ll \ell_e$ where $\Delta r = \|\mathbf{r}_A - \mathbf{r}_B\|$. We show in Fig. 2 the 5 diagrams (γ_1 to γ_{3b}) that are then involved. These contributions only differ from the ones involved in intensity fluctuations (e.g. see Fig. 4 in Ref. [26]) by a change between \mathbf{r}_A and \mathbf{r}_B at the vertex entries. For $\Delta r \gg \ell_e$, $\langle G(\mathbf{r}_A, \mathbf{r}_B) \rangle$ falls exponentially with Δr so that the variance is equal to $\int_V \int_V \langle G(\mathbf{r}, \mathbf{r}_A) G^*(\mathbf{r}', \mathbf{r}_A) G^*(\mathbf{r}, \mathbf{r}_B) G(\mathbf{r}', \mathbf{r}_B) \rangle d^d \mathbf{r} d^d \mathbf{r}'$. In other words, the diagram $\langle \zeta^2 \rangle$ in Fig. 2 vanishes. The diagrams γ_{2b} is short-range in $\mathbf{r}_A, \mathbf{r}_B$ and therefore also vanishes. Because correlation γ_{3b} is long-range only with respect to \mathbf{r}, \mathbf{r}' , it also does not contribute. Diagrams γ_1 and γ_{3a} are also long range but with respect to positions \mathbf{r}_A and \mathbf{r}_B . Because γ_{3a} involves two Hikami boxes, the correlation scales as $1/g^2$ where g is the conductance which is much larger than 1. So it is negligible compared to the zero-order contribution γ_1 that is responsible of Gaussian fluctuations. Thus it seems that γ_1 dominates the NCF fluctuations for a small number of noise sources [18]. Using the same arguments as the one used for intensity fluctuations, it can be shown that γ_1 vanishes when the integrations over \mathbf{r} and \mathbf{r}' are performed over the entire scattering volume. The only contribution to the fluctuations is then the infinite range correlation γ_{2a} . From the mathematical expression of the diagram, we show in a supplemental material [27] that

$$\gamma_{2a} = 2\Delta^4 (\Im \langle G(\mathbf{r}, \mathbf{r}) \rangle)^2 h \left| \int_V L(\mathbf{r}) d^d r \right|^2 \times \frac{K}{D} L(\mathbf{r}_B, \mathbf{r}_A) \Im \langle G(\mathbf{r}_A, \mathbf{r}_A) \rangle \Im \langle G(\mathbf{r}_B, \mathbf{r}_B) \rangle, \quad (4)$$

where h is the Hikami constant and $\Delta = \ell_e/k_0$. Here the Ladder L is solution of the steady state diffusion equation with absorption, i.e., $-D\nabla^2 L(\mathbf{r}) + L(\mathbf{r})c/l_e = K\delta(\mathbf{r})$. For 3D samples, $h = \ell_e^5/48\pi k^2$, $K = 4\pi c/\ell_e^2$ and $D = \ell_e c/3$ and for 2D samples, $h = \ell_e^5/32k^3$, $K = 4k_0/\ell_e$ and $D = \ell_e c/2$. In both cases, Eq. (4) yields,

$$\gamma_{2a} = \frac{l_a^2}{2k_0^2} \langle G(\mathbf{r}_B, \mathbf{r}_A) G^*(\mathbf{r}_B, \mathbf{r}_A) \rangle. \quad (5)$$

The same result is directly obtained when γ is derived from $\langle |\zeta_\infty(\mathbf{r}_A, \mathbf{r}_B)|^2 \rangle$, with ζ_∞ given by Eq. (2). This shows that the NCF is not “self-averaging” in the sense that it does not converge towards the mean Green’s function but towards the *exact* Green’s function. The NCF is therefore sensitive to scatterings that occur at a distance larger than a mean free path from the probes. This fundamental result is crucial in monitoring applications. It indeed shows that it is possible to follow the evolution of a scatterer hidden behind a multiple scattering media [28].

When $\Delta r \ll \ell_e$, Eq. (4) diverges because $L(\mathbf{r}_A, \mathbf{r}_A) \rightarrow \infty$. Indeed, diagram γ_{2a} fails in predicting the effect of a ladder crossing located in one mean free path around the probes. However this is only an artifact effect that is regularized by replacing γ_{2a} by the diagram γ_{0a} (see Fig. 2) in which the Hikami vertex is replaced by a C_0 -like one. The correlation γ_{0a} depends on the details of the local disorder around the probe and involves a non-universal vertex χ_0 [15]. This correlation term is given by $\gamma_{0a} = 2\delta V^2 \Delta^2 (\Im \langle G(\mathbf{r}, \mathbf{r}) \rangle)^2 \left| \int_V L(\mathbf{r}) d^3 r \right|^2 \chi_0$. In case of white-noise disorder (which generally does not hold) at 3D, $\chi_0 = \ell_e/32\pi k_0$ [15].

The correlations γ_{0a} and γ_{2a} can be seen as the two asymptotic regimes $\Delta r \ll \ell_e$ and $\Delta r \gg \ell_e$, respectively, of a unique non-Gaussian NCF correlation that arises in mesoscopic multiple scattering media. Moreover because $\zeta_\infty(\mathbf{r}_A, \mathbf{r}_B)$ and CDOS are both proportional to $\Im \langle G(\mathbf{r}_A, \mathbf{r}_B) \rangle$, CDOS fluctuations also results from the same infinite range correlation γ_{2a} . This result is consistent with the fact that the local density of states is given by C_0 [12, 14]. Indeed when $\mathbf{r}_A = \mathbf{r}_B$, $\zeta_\infty(\mathbf{r}_A, \mathbf{r}_A)$ is proportional to the intensity $I(\mathbf{r}_A)$. Hence, fluctuations of both quantities are dominated by the same diagram γ_{0a} .

We perform numerical simulations to support these derivations. The sample is a 2D multiple scattering medium made of 10^4 isotropic scatterers enclosed in a disk of diameter $100\lambda_0$. Here, $l_a \sim 63\lambda_0$ and $\ell_e \sim 2\lambda_0$.

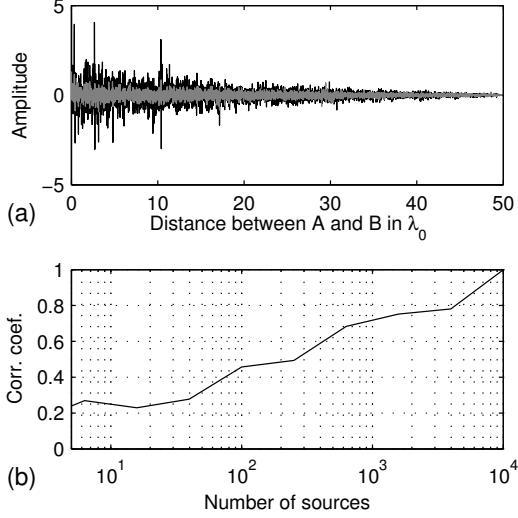


Figure 3. (a) Amplitude of the imaginary part of the cross-correlated field with respect to $\|\mathbf{r}_A - \mathbf{r}_B\|$ for 40 (gray curve) and 10000 (black curve) noise sources. (b) The normalized correlation coefficient for a single realization of disorder between the imaginary parts of the Green's function and ζ obtained for several numbers of noise sources.

Because, the sources are embedded in the multiple scattering media, we have chosen a scattering matrix inversion method rather than the previous time-domain simulation used for Fig. 1. The real part of NCF computed for one realization of disorder is plotted in Fig. 3(a) with respect to Δr for two different number of noise sources. Still for one realization, we show in Fig. 3(b) the normalized spatial correlation coefficient between the imaginary part of the GF and the NCF obtained for a number of noise sources varying from 1 to 10^4 . In this last case, NCF is seen to be exactly equal to $\Im \langle G(\mathbf{r}_A, \mathbf{r}_B) \rangle$.

The variance is estimated in the following from 500 realizations of disorder. The evolution of γ with Δr is shown in Fig. 4. We observe that γ is maximum for $\Delta \mathbf{r} = 0$ due to the γ_{0a} contribution. It first falls rapidly until γ_{0a} vanishes for $\Delta \mathbf{r} \sim \lambda_0/2$. The fluctuations are then seen to decrease as $L(\Delta r) = K_0(\Delta r \sqrt{c/Dl_a})/2\pi D$ which is predicted by Eq. (4). This is a numerical confirmation that γ_{2a} correlation is infinite range.

The condition of an infinite distribution of noise sources is most of the time not fulfilled in seismology and in acoustics. We consider in the following noise sources which illuminate the sample from N independent positions. The NCF fluctuations shown in Fig. 5 with $\Delta r \gg \ell_e$ are computed for N increasing from 1 to 10^4 . For large values of N , γ is seen in Fig. 5 to increase as N^2 . The non-Gaussian contribution γ_{2a} which scales as N^2 indeed overcomes the Gaussian contribution γ_1 which scales as N [18]. Fluctuations γ finally saturates here for $N \sim 10^4$ because the sample is already illuminated from all the incident directions of space.

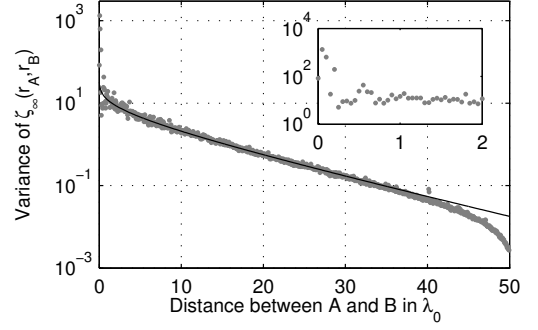


Figure 4. Variance of $\zeta_\infty(\mathbf{r}_A, \mathbf{r}_B)$ with respect to the distance between \mathbf{r}_A and \mathbf{r}_B . The simulation parameters are the same as the ones used in Fig. 5 with 10^4 sources. This variance is estimated from 500 realizations of the disorder. The black line is a fit of the simulation results with Eq. (4) where Ladder L is the solution of the 2D diffusion equation with losses.

Fluctuations of the NCF are seen in Fig. 5 to be enhanced for a few sources $N \sim 1$. This indicates that in addition to γ_1 other diagrams are contributing to γ . When $N = 1$, paths crossing occurs in the vicinity of the noise source location \mathbf{r}_S and another C_0 correlation has to be taken into account. To this end, we introduce the diagram γ_{0b} shown in Fig. 2. Its mathematical expression is

$$\gamma_{0b} = 2\delta V^2 \Delta^2 L(\mathbf{r}_B, \mathbf{r}_S) L(\mathbf{r}_A, \mathbf{r}_S) \times \Im \langle G(\mathbf{r}_A, \mathbf{r}_A) \rangle \Im \langle G(\mathbf{r}_B, \mathbf{r}_B) \rangle \chi_0. \quad (6)$$

Here δV is the volume of the single source that is assumed smaller than l_e^3 . To complete our analysis, we note that in the case of $\Delta r \ll l_e$ and a single noise source, γ is given by the sum of the two C_0 diagrams[29] shown in fig. 2. Then $\gamma = 2\delta V^2 \Delta^2 |L(\mathbf{r}_A, \mathbf{r}_S)|^2 \chi_0 (\Im \langle G(\mathbf{r}_A, \mathbf{r}_A) \rangle^2 + \Im \langle G(\mathbf{r}_S, \mathbf{r}_S) \rangle^2)$. Those considerations confirm the intuitive result that fluctuations of NCF caused by a source located inside a multiple scattering medium are stronger than fluctuations caused by a source outside this disordered medium which only involves Gaussian fluctuation.

In conclusion, we have demonstrated that in a multiple scattering medium the scatterers act as secondary sources so that the noise cross-correlation function measured between two probes converges towards the imaginary part of the mean Green's function even though the medium is illuminated by a single source. We have also shown that the NCF is not self averaging with the number of noise sources. Increasing the spatial diversity of noise field does not make the NCF converge towards the imaginary part of the mean GF but towards the imaginary part of the exact GF. This has been demonstrated by deriving the variance of the NCF in the case of equipartition. More generally, non-Gaussian correlations that contribute to

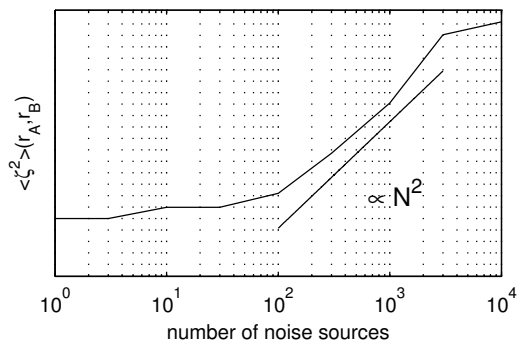


Figure 5. Fluctuation of the NCF for positions A and B that are distant of more than a wavelength (continuous line). The result is obtained from a 2D scattering matrix inversion with 10000 scatterers. Results for 1 to 3000 sources (resp. 10000) is obtained from 5e5 averaging (resp. 500 averaging).

the mesoscopic fluctuations have been identified.

Those results are situated at the crossroads between fundamental physics and applied physics in many different fields such as seismology, acoustics, microwave, optics or material science. In acoustics and in seismology, the estimation of the NCF is easily performed by the direct cross-correlation of recorded time-dependent fields. However, the noise sources are usually not uniformly distributed. On the other hand, in optics, one can take benefit of the thermal noise that is uniform at thermal equilibrium. But then it is more tedious to measure NCF. In material science, metallic nanostructures can for instance be excited with surface plasmons in disordered media. Measuring the NCF at thermal equilibrium would make possible to estimate the CDOS. We suggest the experiment consisting in the measurement of the field intensity diffracted by two tips on a metallic surface at thermal equilibrium where plasmons are multiply scattered. This would be an extension of thermal radiation scanning tunneling microscopy[30].

The authors want to thanks Roger Maynard, Philippe Roux and Remi Carminati for fruitful discussions. This work have been partially supported by ANR grant ANR-10-BLAN-0124 OPTRANS.

* julien.derosny@espci.fr

- [1] R.L. Weaver and O.I. Lobkis, Phys. Rev. Lett. **87**, 134301 (2001), ISSN 0031-9007.
- [2] H. Callen and T. Welton, Phys. Rev. **83**, 34 (1951), ISSN 0031-899X.
- [3] K. Wapenaar, E. Slob, and R. Snieder, Phys. Rev. Lett.

- 97**, 234301 (2006), ISSN 0031-9007.
- [4] M. Campillo and A. Paul, Science **299**, 547 (2003), ISSN 0036-8075.
- [5] N. Shapiro, M. Campillo, L. Stehly, and M. Ritzwoller, Science **307**, 1615 (2005), ISSN 0036-8075.
- [6] P. Roux, W. Kuperman, and N. Grp, J. Acoust. Soc. Am. **116**, 1995 (2004), ISSN 0001-4966.
- [7] R. L. Weaver and O. I. Lobkis, J. Acoust. Soc. Am. **113**, 2611 (2003).
- [8] K. Wapenaar, Phys. Rev. Lett. **93**, 254301 (2004), ISSN 0031-9007.
- [9] M. Davy, M. Fink, and J. de Rosny, Phys. Rev. Lett. **110**, 203901 (2013).
- [10] A. Derode, E. Larose, M. Tanter, J. de Rosny, A. Tourin, M. Campillo, and M. Fink, J. Acoust. Soc. Am. **113**, 2973 (2003), ISSN 0001-4966.
- [11] A. Mirlin, Phys. Rep. **326**, 259 (2000).
- [12] B.A. van Tiggelen and S.E. Skipetrov, Phys. Rev. E **73**, 045601 (2006).
- [13] M.D. Birowosuto, S.E. Skipetrov, W.L. Vos, and A.P. Mosk, Phys. Rev. Lett. **105**, 013904 (2010).
- [14] A. Cazé, R. Pierrat, and R. Carminati, Phys. Rev. A **82**, 043823 (2010).
- [15] B. Shapiro, Phys. Rev. Lett. **83**, 4733 (1999).
- [16] E. Akkermans and G. Montambaux, *Mesoscopic physics of electrons and photons* (Cambridge University Press, 2007).
- [17] B.A. van Tiggelen, Phys. Rev. Lett. **91**, 243904 (2003), ISSN 0031-9007.
- [18] E. Larose, L. Margerin, A. Derode, B. van Tiggelen, M. Campillo, N. Shapiro, A. Paul, L. Stehly, and M. Tanter, Geophys. **71**, S111 (2006).
- [19] G. Bal, G. Papanicolaou, and L. Ryzhik, Stoch. Dyn. **2**, 507 (2002).
- [20] R. L. Weaver and O. I. Lobkis, J. Acoust. Soc. Am. **116**, 2731 (2004).
- [21] J. de Rosny and M. Davy, *Movie of the cross-correlated mean field*, Electronic, URL http://ftp.espci.fr/shadow/article_rosny_davy/movie.avi, (2013).
- [22] This relation [16] is similar to Eq. (2) but the elastic mean free path replaces the absorption mean free path because the attenuation of mean field is mainly due to elastic scattering.
- [23] A. Derode, E. Larose, M. Campillo, and M. Fink, Appl. Phys. Lett. **83**, 3054 (2003), ISSN 0003-6951.
- [24] M. Davy, Z. Shi, and A. Z. Genack, Phys. Rev. B **85**, 035105 (2012).
- [25] The variance of a self-averaging quantity should fall towards 0 when the quantity is integrated over time or space.
- [26] R. Berkovits and S. Feng, Phys. Rep. **238**, 135 (1994).
- [27] J. de Rosny and M. Davy, *Supplementary material : full derivation of the γ_{2a} contribution*.
- [28] L. Bonneau, C. Prada, M. Fink, and A. Tourin, Waves in Random and Complex Media **22**, 109 (2012).
- [29] A. Retzker and B. Shapiro, Pramana **58**, 225 (2002).
- [30] Y. De Wilde, F. Formanek, R. Carminati, B. Gralak, P.-A. Lemoine, K. Joulain, J.-P. Mulet, Y. Chen, and J.-J. Greffet, Nature **444**, 740 (2006).

Supplemental material of “Green’s function retrieval and
fluctuations of the cross density of states in multiple scattering
media”

Julien de Rosny and Matthieu Davy

Institut Langevin, ESPCI, CNRS, 1 rue Vauquelin, 75231 Paris cedex 05. and

Institut d’Electronique et de Télécommunications de Rennes,

University of Rennes 1, Rennes 35042, France.

(Dated: 04/09/2013)

Abstract

In this supplemental material, we derive the γ_{2a} correlation term shown in Fig. 2 of the main article.

The variance γ of the noise cross-correlation function ζ_V is given by

$$\gamma = \int_V \int_V \langle G(\mathbf{r}, \mathbf{r}_A) G^*(\mathbf{r}', \mathbf{r}_A) G^*(\mathbf{r}, \mathbf{r}_B) G(\mathbf{r}', \mathbf{r}_B) \rangle d^d \mathbf{r} d^d \mathbf{r}' - \left| \int_V \langle G(\mathbf{r}, \mathbf{r}_A) G^*(\mathbf{r}', \mathbf{r}_B) \rangle d^d \mathbf{r} \right|^2.$$

where d is the space dimension. For simplicity, we have replaced S_V by an integration over a finite volume V (which is a surface at 2D).

The mathematical expression of the correlation γ_{2a} shown in Fig. 2 integrated over \mathbf{r} and \mathbf{r}' is given by

$$\gamma_{2a} = 2\Delta^4 \Im \langle G(\mathbf{r}_A, \mathbf{r}_A) \rangle \Im \langle G(\mathbf{r}_B, \mathbf{r}_B) \rangle \times \iiint \Im \langle G(\mathbf{r}, \mathbf{r}) \rangle \Im \langle G(\mathbf{r}', \mathbf{r}') \rangle H L(s, r_A) L(s, r_B) L(s, r) L(s, r') d^d r d^d r' d^d s.$$

Here H is the differential operator of the Hikami vertex. It is given by [1] $H = -h(2\nabla_{r_A} \cdot \nabla_{r_B} + 2\nabla_r \cdot \nabla_{r'} + \nabla_r \cdot \nabla_{r_B} + \nabla_r \nabla_{r_A} + \nabla_{r'} \cdot \nabla_{r_A} + \nabla_{r'} \nabla_{r_B})$, where h is the Hikami constant and $\Delta = l_e/k$. Six integrals have to be evaluated. Due to the divergence theorem, the five volume integrals that involve ∇_r or $\nabla_{r'}$ can be expressed as surface integrals, $\int_V \nabla_r L(s, r) d^d r = \int_{A(V)} L(s, r) d^{d-1} r$, where $A(V)$ is a surface enclosing the volume V . Because the medium is slightly lossy, the ladder L falls exponentially with the integration volume so that $\int_{A(V)} L(s, r) d^{d-1} r = 0$. Consequently only the first term in Eq. (2) contributes to γ_{2a} .

$$\gamma_{2a} = 2h\Delta^4 \int_V \int_{V'} \Im \langle G(\mathbf{r}, \mathbf{r}) \rangle \Im \langle G(\mathbf{r}', \mathbf{r}') \rangle \Im \langle G(\mathbf{r}_A, \mathbf{r}_A) \rangle \Im \langle G(\mathbf{r}_B, \mathbf{r}_B) \rangle \times L(\mathbf{r}, s) L(\mathbf{r}', s) [\nabla L(\mathbf{r}_A, s) \nabla L(\mathbf{r}_B, s)] d^d r d^d r' d^d s.$$

The mean value $\Im \langle G(\mathbf{r}, \mathbf{r}) \rangle$ is a constant equals to $k_0/4\pi$ in 3D and $1/4$ in 2D. So the previous expression becomes

$$\gamma_{2a} = 2h\Delta^4 \left(\Im \langle G \rangle \int_V L(\mathbf{r}) d^d r \right)^2 \int_V \int_{V'} \Im \langle G(\mathbf{r}_A, \mathbf{r}_A) \rangle \Im \langle G(\mathbf{r}_B, \mathbf{r}_B) \rangle [\nabla L(\mathbf{r}_A, s) \nabla L(\mathbf{r}_B, s)] d^d s. \quad (1)$$

The integral $\int_V L(\mathbf{r}) d^d r$ is equal to $K\tau_a$, i.e., Kl_a/c .

The gradient product is given by

$$\begin{aligned} 2\nabla L(\mathbf{r}_B, s) \nabla L(\mathbf{r}_A, s) &= \nabla [L(\mathbf{r}_A, s) \nabla L(\mathbf{r}_B, s) + L(\mathbf{r}_B, s) \nabla L(\mathbf{r}_A, s)] \\ &\quad - L(\mathbf{r}_A, s) \nabla^2 L(\mathbf{r}_B, s) - L(\mathbf{r}_B, s) \nabla^2 L(\mathbf{r}_A, s). \end{aligned} \quad (2)$$

Because the Ladder L is solution of the diffusion equation,

$$-D\nabla^2 L(\mathbf{r}_1 - \mathbf{r}_2) + L(\mathbf{r}_1 - \mathbf{r}_2)/\tau_a = K\delta(\mathbf{r}_1 - \mathbf{r}_2),$$

Eq. (2) can be expressed as,

$$\begin{aligned} 2\nabla L(\mathbf{r}_A, s) \nabla L(\mathbf{r}_B, s) &= -L(\mathbf{r}_A, s) \left[\frac{1}{D\tau_A} L(\mathbf{r}_B, s) - \frac{K}{D} \delta(\mathbf{r}_B - s) \right] \\ &\quad - L(\mathbf{r}_B, s) \left[\frac{1}{D\tau_A} L(\mathbf{r}_A, s) - \frac{K}{D} \delta(\mathbf{r}_A - s) \right]. \end{aligned}$$

The integration over volume V leads to

$$2 \int_V \nabla L(\mathbf{r}_A, s) \nabla L(\mathbf{r}_B, s) d^d s = \frac{K}{D} [L(\mathbf{r}_A, \mathbf{r}_B) + L(\mathbf{r}_B, \mathbf{r}_A)].$$

because at $3D\frac{1}{\tau_a} \int_V L(\mathbf{r}_A, s) L(\mathbf{r}_B, s) d^d s < \frac{1}{\tau_a} \int_V L^2(\mathbf{r}_A, s) d^3 s \sim \frac{K^2}{D^2\tau_a} \sqrt{D\tau_a}$. So when $\tau_A \rightarrow \infty$, the integral goes toward 0. At 2D, the demonstration is much more difficult because $\int L^2(\mathbf{r}_A, s) d^2 s$ scales as τ_A but the result is identical.

We then use that diffusion is a reciprocal process, $L(\mathbf{r}_A, \mathbf{r}_B) = L(\mathbf{r}_B, \mathbf{r}_A)$. The previous expression can therefore be simplified into

$$\int_V \nabla L(\mathbf{r}_A, s) \nabla L(\mathbf{r}_B, s) d^3 s = \frac{K}{D} L(\mathbf{r}_A, \mathbf{r}_B).$$

It finally comes,

$$\gamma_{2a} = 2h\Delta^4 \left(\Im \langle G \rangle \int_V L(\mathbf{r}) d^d r \right)^2 \Im \langle G(\mathbf{r}_A, \mathbf{r}_A) \rangle \Im \langle G(\mathbf{r}_B, \mathbf{r}_B) \rangle \frac{K}{D} L(\mathbf{r}_A, \mathbf{r}_B). \quad (3)$$

[1] R. Berkovits and S. Feng, Phys. Rep. **238**, 135 (1994),

<http://www.sciencedirect.com/science/article/pii/0370157394900795>